AUT Journal of Electrical Engineering

AUT J. Elec. Eng., 52(2) (2020) 193-204
DOI: 10.22060/eej.2020.17665.5324

Nonlinear Robust Tracking Control of an Underwater Vehicle-Manipulator System

Mozhde Mahmoodi[1], Amir Farhad Ehyaei[1,*], Javad Ehyaei[2]

[1] Department of Electrical Engineering, Imam Khomeini International University, Qazvin, Iran
[2] Department of Mechanical Engineering, Imam Khomeini International University, Qazvin, Iran

ABSTRACT: This paper develops an improved robust multi-surface sliding mode controller for a complicated five degrees of freedom Underwater Vehicle-Manipulator System with floating base. The proposed method combines the robust controller with some corrective terms to decrease the tracking error in transient and steady state. This approach improves the performance of the nonlinear dynamic control scheme and makes the states stable even in presence of unknown effects of hydrodynamic disturbances and unmodelled dynamics. In this regard, the dynamic model of an UVMS is extracted using the Newton–Euler formulation which has been validated by using an ADAMS 3-D model. The control algorithm is based on Lyapunov technique and is able to provide the stability of the whole system during tracking of the desired trajectory with an acceptable precision. The controller parameters are also optimized utilizing the concept of Genetic Algorithm with the aim of increasing the speed of system while decreasing the tracking error which leads to bounded control inputs. Finally, the efficacy of the control scheme, is compared with other conventional methods and the simulation results show the short settling time, low and smooth control effort and asymptotic stability of the states as well as the sliding surfaces of the proposed controller.

Review History:

Received: 2020-01-06
Revised: 2020-04-15
Accepted: 2020-06-28
Available Online: 2020-12-01

Keywords:

Underwater Vehicle-Manipulator System
Multi-surface sliding mode
Robust control
External disturbance, Model uncertainty

1.INTRODUCTION

In recent few decades, the underwater vehicle manipulator systems (UVMS) have attracted various scientific research and industrial exploitation in the field of welding, nondestructive test of marine structures or underwater oil and gas pipelines for closing and opening of valves, drilling, cutting, sampling, and installing ocean sampling devices and discovery [1,2].

In such applications, changes in velocity and position of the UVMS system over time are highly affected by its dynamical structure. In this regard, two different approaches can be seen in the literature to analyze the configuration of the system. The first method is described in [3] which authors considered the UVMS as two independent subsystems: manipulator and vehicle. The equations of motion for each subsystem is expanded and the interaction forces between subsystems are added to these equations. The second method is to consider the UVMS as a single body [4]. In other hand, modeling a proper control method for stabilization of UVMS is a very challenging issue because of the existence of highly nonlinear couplings and unknown external time-varying disturbances and complexity of parametric uncertainties. To overcome these challenges, several control methods have been investigated and proposed so far. For instance, the authors in [5-7] described complexity of underwater manipulators dynamic in presence of hydrodynamic disturbances and presented an indirect adaptive control method for a model of UVMS. Also, researchers in [8] proposed a control strategy to consider the effect of drag forces on the whole underwater system and in [9] an adaptive tracking controller based on the virtual decomposition has been presented.

*Corresponding author's email: f.ehyaei@eng.ikiu.ac.ir

On the other hand, some papers focus on hybrid controllers to generate acceptable performance of under water system. For example, authors in [10,11] designed a sliding mode controller (SMC) based on fuzzy method and in [12] a PID sliding surface is used to show better performance of UVMS in trajectory tracking. Also, in [13] the authors proposed a robust single-input fuzzy logic control method for the task space control problem of an UVMS against uncertain dynamics and disturbances. In another work [14], researchers proposed a feed forward controller along with a disturbance estimator based on PID-like fuzzy logic control law to develop the closed loop stability of the UVMS system. The other controller which has been implemented on the UVMS system is time delay estimation. The authors in [15,16] applied this method based on a nonlinear robust controller such as feedback linearization to solve the trajectory tracking control problem of underwater system.

This paper, presents an improved robust controller based on multi surfaces sliding mode method for a float-base UVMS with five degrees of freedom. The proposed method has several superiorities over other works, which can be taken into account as follows:

a) In this paper, a multi-surface sliding mode controller will be improved by utilizing some PID correction terms in the sliding surfaces. Advantage of the presented multi surface integral sliding mode controller (MS-ISMC) is that it is insensitive to the modelling errors, parameter uncertainties and other disturbances, and it can improve the steady-state response of the system as well. Also, the chattering of the controller is reduced rather than conventional sliding mode controller. The simulation results show that the proposed controllers can achieve better robustness and tracking capability in comparison with the SMC controller.

b) Despite the other pervious works, this paper considers full dynamic of an UVMS with floating base including drag and Buoyant forces, system uncertainties and external disturbances. The proposed controller, based on this model, is an effectual controller especially when the end-effector interacts with the environment in presence of hydrodynamic disturbances.

Also, this study optimizes the controller parameters utilizing the concept of Genetic Algorithm. The aim of the proposed method is to increase the speed of converging to the desired trajectory while decreasing the tracking error and to achieve a bounded control input in comparison with other conventional approaches. The obtained results show acceptable performance of the proposed control scheme.

This paper is organized as follows: In Section 2, the full dynamic of a floating base UVMS is extracted. The improved robust and accurate multi surfaces integral SMC is presented in Section 3. The results from numerical simulations are discussed in Section 4 and finally in Section 5 conclusions on the present paper are driven.

2.DYNAMIC MODEL OF THE UVMS

The UVMS in this study is a five-DOF floating base manipulator system as shown in Fig.1. E (x_u,y_u) is the Earth-fixed (inertial) frame, B (x_0,y_0) is the base frame (moving), M_1 (x_1,y_1) and M_2 (x_2,y_2) are manipulator frame of Link1 and Link2.

Drag forces in our floating base UVMS consist of three parts. The first part is a drag force deduced from the floating base in four directions. The second and third parts are drag forces exerted on link1 and link2 of the manipulator respectively [6,17]. The equations associated with these drag forces are extracted using Maple software as following:

$$\begin{cases} F_{D_{01}} = \frac{1}{2}\,\rho\, C_d L_{z0} \int_0^{L_{y0}} (V_{P_{x_0}}[x])^2\, dy_0 \\ F_{D_{02}} = \frac{1}{2}\,\rho\, C_d L_{z0} \int_0^{L_{y0}} (V_{P_{x_0}}[y])^2\, dy_0 \\ F_{D_{03}} = \frac{1}{2}\,\rho\, C_d L_{z0} \int_0^{L_{x0}} (V_{P_{y_0}}[x])^2\, dx_0 \\ F_{D_{04}} = \frac{1}{2}\,\rho\, C_d L_{z0} \int_0^{L_{x0}} (V_{P_{y_0}}[y])^2\, dx_0 \end{cases} \tag{1}$$

$$\begin{cases} F_{D_{11}} = \frac{1}{2}\,\rho\, C_d L_{z1} \cdot \int_0^{L_1} (V_{p_1}[y])^2\, dx_1 \\ F_{D_{12}} = \frac{1}{2}\,\rho\, C_d L_{z1} \cdot \int_0^{L_1} (V_{p_1}[x])^2\, dx_1 \end{cases} \tag{2}$$

$$\begin{cases} F_{D_{21}} = \frac{1}{2}\,\rho\, C_d L_{z2} \cdot \int_0^{L_2} (V_{p_2}[y])^2\, dx_2 \\ F_{D_{22}} = \frac{1}{2}\,\rho\, C_d L_{z2} \cdot \int_0^{L_2} (V_{p_2}[x])^2\, dx_2 \end{cases} \tag{3}$$

where C_d is drag coefficient, L_{x0} and L_{y0} are width and length of the base and L_{zi} is height of $Link_i$ (L_{z0} is height of the base),$V_{P_{x_0}}[x]$ and $V_{P_{x_0}}[y]$ are translational velocities of x_0 point;$V_{P_{y_0}}[x]$ and $V_{P_{y_0}}[y]$ are translational velocities of y_0 point; $V_{p_1}[x]$ and $V_{p_1}[y]$ are velocities of x_1 and y_1 points; $V_{p_2}[x]$ and $V_{p_2}[y]$ are velocities of x_2 and y_2 points and ρ is fluid density. Therefore, the total drag forces applied on floating base of UVMS is established as:

$$D=[F_{D_{0r}} \quad F_{D_{1b}} \quad F_{D_{2C}}] \tag{4}$$

where $F_{D_{0r}}$ (r=1,2,3,4), $F_{D_{1b}}$(b=1,2) and $F_{D_{2C}}$(c=1,2) are drag forces of base, Link1 and Link2 respectively.

When an UVMS is partially or fully submerged in ocean, an upward force is exerted by the water on to it, called the buoyancy force. The acting buoyant force on the UVMS is equal to the mass of displaced water [6,18]. Direction of buoyant force is in opposite direction of gravitational force. Therefore, the buoyant forces acting on base (link0), link1 and link2 are directed up and equal to:

$$\begin{cases} B_0 = L_{x0} \cdot L_{z0} \cdot L_{y0} \cdot g \cdot \rho \\ B_1 = L_{x1} \cdot L_{z1} \cdot L_{y1} \cdot g \cdot \rho \\ B_2 = L_{x2} \cdot L_{z2} \cdot L_{y2} \cdot g \cdot \rho \end{cases} \tag{5}$$

$$B=[B_0 \quad B_1 \quad B_2] \tag{6}$$

where g is the gravitational acceleration vector, L_{xi} is width of $Link_i$ and L_{yi} is length of the link in y direction.

Now, by using Eqs. (1)-(6), the final form of dynamic equations of the UVMS can be derived as [19]:

$$u = M(q)\ddot{q} + V(\dot{q}\,.q)\dot{q} + G(q) + D(\dot{q}\,.q)\dot{q} + B(q) + d(t) \tag{7}$$

where $q \in \boldsymbol{R^n}$ is the vector of joint variables and $u \in \boldsymbol{R^n}$ is the vector of torques acting at the joints. $M(q) \in \boldsymbol{R^{n\times n}}$ is the symmetric positive definite inertia matrix which is bounded for any q, $V(\dot{q}\,.q)q \in \boldsymbol{R^n}$ represents the centrifugal and Coriolis torques, $G(q) \in \boldsymbol{R^n}$ is the vector of gravitational torques, $D(\dot{q}\,.q)\dot{q} \in \boldsymbol{R^n}$ is the vector of damping (hydrodynamic) effects of manipulator, $B(q) \in \boldsymbol{R^n}$

is the buoyancy force $d(t)$ is the vector of unknown disturbances which includes both system uncertainties and external disturbances. The first three terms of (7) are in the form:

$$M(q) = \begin{pmatrix} -24\, sin(\theta_1)\, Ra_1 m_1 + \cdots & \cdots & \cdots \\ \vdots & \ddots & \vdots \\ \vdots & \cdots & -L_1\, cos(\theta_2)\, a_2 m_2 + \cdots \end{pmatrix}_{5\times5} \quad (8)$$

$$V(\dot{q}\,.q) = \begin{bmatrix} -6\dot{\theta}_0(t)^2 L_0\, sin(\theta_1(t))\, a_1 m_1 + \cdots \\ \vdots \\ -L_0\dot{\theta}_0(t)^2\, sin(\theta_1(t)+\theta_2(t))\, a_2 m_2 + \cdots \end{bmatrix}_{5\times1} \quad (9)$$

$$G(q) = \begin{bmatrix} -12L_0\, cos(\theta_0(t))\, m_1 + \cdots \\ \vdots \\ -a_2 m_2\, cos(-\theta_2(t)+\theta_0(t)-\theta_1(t)) + \cdots \end{bmatrix}_{5\times1} \quad (10)$$

in which m_i is the mass of link$_i$ (m_0 is the mass of base), also,is θ_i relative joint angle (θ_0 is angle of base), L_i is length of link$_i$ (L_0 is distance between the center of base and link1), a_i is position vector from joint i to the center of gravity, R is length from origin of x_0, y_0 to thruster and F_j is thruster force ($j = 1,2,3$).

Now, by using the rigid-body dynamic model in (7) one can write:

$$\ddot{q} = \alpha(q) + \beta(q)u \quad (11)$$

in which:

$$\alpha(q) = M(q)^{-1}[(-V(\dot{q}\,.q)\dot{q} - G(q) - D(\dot{q}\,.q)\dot{q} - B(q) - d(t))]_{5\times1} \quad (12)$$

$$\beta(q) = [M(q)^{-1}]_{5\times5} \quad (13)$$

At last, the state space model of the UVMS system, $\dot{Z} = f(Z, u)$, is defined as:

$$Z = [z_1, \ldots, z_{10}] = [\theta_0, \dot{\theta}_0, \theta_1, \dot{\theta}_1, \theta_2, \dot{\theta}_2, x, \dot{x}, y, \dot{y}] \quad (14)$$

$$f(Z,u) = \begin{pmatrix} z_2 \\ \alpha_1 + \beta_{11}u_1 + d_{\theta0} \\ z_4 \\ \alpha_2 + \beta_{22}u_2 + d_{\theta1} \\ z_6 \\ \alpha_3 + \beta_{33}u_3 + d_{\theta2} \\ z_8 \\ \alpha_4 + \beta_{44}u_4 + d_x \\ z_{10} \\ \alpha_5 + \beta_{55}u_5 + d_y \end{pmatrix} \quad (15)$$

Assumption 1. In general, the disturbance vector $d(t) = [d_{\theta0}, \ldots, d_y]$ is assumed to be a bounded uncertainty, i.e. $|d(t)| \le \delta$ where ä is positive constant.

Assumption 2. System uncertainties is written as:

$$M = M_0 + \Delta M\ ,\ V = V_0 + \Delta V$$
$$G = G_0 + \Delta G\ ,\ D = D_0 + \Delta D \quad (16)$$

where $\Delta M, \Delta V, \Delta D$ and ΔG areuncertaintiesrepresenting parameter variations, $M_0(q), V_0(q,\dot{q}), G_0(q)$ and $D_0(q,\dot{q})$ are nominal terms and uncertainties are bounded such that $\Delta M_l \le |\Delta M| \le \Delta M_h$, $\Delta V_l \le |\Delta V| \le \Delta V_h$, $\Delta G_l \le |\Delta G| \le \Delta G_h$ and $\Delta D_l \le |\Delta D| \le \Delta D_h$. The subscripts l and h denote lower and upper uncertainty values.

Based on this assumption, (7) can be rearranged as:

$$\ddot{q} = (M_0 + \Delta M)(q)^{-1}(u - (G_0 + \Delta G)(q) - (V_0 + \Delta V)(\dot{q}\,.q)\dot{q} - (D_0 + \Delta D)(\dot{q}\,.q)\dot{q} - B(q) - d(t)) \quad (17)$$

3.MULTI-SURFACE SLIDING MODE CONTROLLER WITH INTEGRAL CORRECTIVE TERM IN THE SLIDING SURFACE

The purpose of this section is to combine multi surfaces sliding mode control method with some correcting terms in order to develop a robust solution. This solution increases the rate of error convergence to zero and decreases the tracking error in transient and steady state to improve the performance of the proposed non-linear dynamic control scheme. The SMC method consists of two phases: (a) defining multi sliding surfaces to reach the desired system behavior (acceptable tracking performance); and (b) defining a control law to move the system toward the sliding surface. In this regard, a PID surface can be selected in the error space as follows [20,21]:

$$s_\ell(t) = K_{p\ell}e(t) + K_{i\ell}\int e(\xi)d\xi + K_{d\ell}\frac{d}{dt}e(t) \quad ,\ell = 1,..,5. \quad (18)$$

where $e(t) = z_d(t) - z(t)$ is the tracking error and $K_{p\ell}$, $K_{i\ell}$ and $K_{d\ell}$ are constant and positive definite gain matrices, defined as:

$$K_{p\ell} = diag\{K_{p1}, K_{p2}, K_{p3}, K_{p4}, K_{p5}\}$$
$$K_{d\ell} = diag\{K_{d1}, K_{d2}, K_{d3}, K_{d4}, K_{d5}\} \quad (19)$$
$$K_{i\ell} = diag\{K_{i1}, K_{i2}, K_{i3}, K_{i4}, K_{i5}\}$$

Taking the derivative of sliding surface in (18), gives:

$$\dot{s}_\ell(t) = K_{p\ell}\dot{e}(t) + K_{i\ell}e(t) + K_{d\ell}\ddot{e}(t) = K_{p\ell}\dot{e} + K_{i\ell}e + K_{d\ell}\left[\ddot{q}_d - \alpha(q) - \beta(q)u_\ell(t)\right] \quad (20)$$

$$s\dot{_{\theta_0}}(t) = -K_{d_1}((\beta_{11} + \Delta\beta_{11})u_1(t) + (\alpha_1 + \Delta\alpha_1)) + K_{d_1}\ddot{q}_{d_1} + K_{p_1}\dot{e}_1 + K_{i_1}\ e_1 = 0 \tag{21}$$

$$s\dot{_{\theta_1}}(t) = -K_{d_2}((\beta_{22} + \Delta\beta_{22})u_2(t) + (\alpha_2 + \Delta\alpha_2)) + K_{d_2}\ddot{q}_{d_2} + K_{p_2}\dot{e}_2 + K_{i_2}\ e_2 = 0 \tag{22}$$

$$s\dot{_{\theta_2}}(t) = -K_{d_3}((\beta_{33} + \Delta\beta_{33})u_3(t) + (\alpha_3 + \Delta\alpha_3)) + K_{d_3}\ddot{q}_{d_3} + K_{p_3}\dot{e}_3 + K_{i_3}\ e_3 = 0 \tag{23}$$

$$s\dot{_x}(t) = -K_{d_4}((\beta_{44} + \Delta\beta_{44})u_4(t) + (\alpha_4 + \Delta\alpha_4)) + K_{d_4}\ddot{q}_{d_4} + K_{p_4}\dot{e}_4 + K_{i_4}\ e_4 = 0 \tag{24}$$

$$s\dot{_y}(t) = -K_{d_5}((\beta_{55} + \Delta\beta_{55})u_5(t) + (\alpha_5 + \Delta\alpha_5)) + K_{d_5}\ddot{q}_{d_5} + K_{p_5}\dot{e}_5 + K_{i_5}\ e_5 = 0 \tag{25}$$

Now, considering zero uncertainty $\left(d(t)=0\right)$, the control signal is:

$$u_{eq\ell}(t) = (K_{d\ell}\beta(q))^{-1}\left[k_{P\ell}\dot{e} + K_{i\ell}e + K_{d\ell}\left(\ddot{q}_d - \alpha(q)\right)\right] \tag{26}$$

$$u_{eq1}(t) = \frac{1}{(\beta_{11} + \Delta\beta_{11})}\left(-(\alpha_1 + \Delta\alpha_1) + \dot{z}_{d_2} - \frac{K_{p_1}}{K_{d_1}}(z_2 - z_{d_2}) - \frac{K_{i_1}}{K_{d_1}}(z_1 - z_{d_1})\right) \tag{27}$$

$$u_{eq2}(t) = \frac{1}{(\beta_{22}+\Delta\beta_{22})}\left(-(\alpha_2 + \Delta\alpha_2) + \dot{z}_{d_4} - \frac{K_{p_2}}{K_{d_2}}(z_4 - z_{d_4}) - \frac{K_{i_2}}{K_{d_2}}(z_3 - z_{d_3})\right) \tag{28}$$

$$u_{eq3}(t) = \frac{1}{(\beta_{33}+\Delta\beta_{33})}\left(-(\alpha_3 + \Delta\alpha_3) + \dot{z}_{d_6} - \frac{K_{p_3}}{K_{d_3}}(z_6 - z_{d_6}) - \frac{K_{i_3}}{K_{d_3}}(z_5 - z_{d_5})\right) \tag{29}$$

$$u_{eq4}(t) = \frac{1}{(\beta_{44}+\Delta\beta_{44})}\left(-(\alpha_4 + \Delta\alpha_4) + \dot{z}_{d_8} - \frac{K_{p_4}}{K_{d_4}}(z_8 - z_{d_8}) - \frac{K_{i_4}}{K_{d_4}}(z_7 - z_{d_7})\right) \tag{30}$$

$$u_{eq5}(t) = \frac{1}{(\beta_{55}+\Delta\beta_{55})}\left(-(\alpha_5 + \Delta\alpha_5) + \dot{z}_{d_{10}} - \frac{K_{p_5}}{K_{d_5}}(z_{10} - z_{d_{10}}) - \frac{K_{i_5}}{K_{d_5}}(z_9 - z_{d_9})\right) \tag{31}$$

But, if unanticipated turbulence of parameter variations or unknown external disturbance appears, the control signal cannot guarantee the control performance [20]. Hence, by using an ancillary control scheme named a reaching control law, $u_r(t)$, we not only improve the system performance, but also make it robust against external disturbances. Totally, the MS-ISMC law can be represented as:

$$u_\ell(t) = u_{eq\ell}(t) + u_r(t) \tag{32}$$

To extract the reaching control signal, consider a candidate Lyapunov function as follows:

$$V(t) = \tfrac{1}{2}s^T(t)s(t) = \tfrac{1}{2}\left[s_{\theta_0}^T(t)\cdot s_{\theta_0}(t) + s_{\theta_1}^T(t)\cdot s_{\theta_1}(t) + s_{\theta_2}^T(t)\cdot s_{\theta_2}(t) + s_x^T(t)\cdot s_x(t) + s_y^T(t)\cdot s_y(t)\right] \tag{33}$$

with $V(0)=0$ *and* $V(t)>0$ *for* $s_\ell(t)\neq 0$.

From (33) and considering the following condition:

$$\dot{V}(t) = s_\ell^T(t)\dot{s}_\ell(t) < 0, \quad s_\ell(t)\neq 0 \tag{34}$$

system states will reach the sliding surface, $s_\ell(t)=0$, in finite time; so, the control approach guarantees asymptotic stability of the overall system [20,21]. Now, by substituting (17) and (18) into (34), one can write:

$$s_\ell^T\dot{s_\ell} = s_\ell^T\{K_{p\ell}\dot{e} + K_{i\ell}e + K_{d\ell}\ddot{q}_d + K_{d\ell}(M_0 + \Delta M)^{-1}\left((\Delta V + V_0 + \Delta D + D_0)\dot{q} + \Delta G(q) + G_0 + B(q) + d(t)\right\} - s_\ell^T K_{d\ell}(M_0 + \Delta M)^{-1}\left(u_{eq_\ell} + u_r\right) \tag{35}$$

Then, from (26) and after some simplification, we have:

$$s_\ell^T\dot{s_\ell} = s_\ell^T\{K_{d\ell}[|\Delta V - M_0^{-1}V_0\Delta M + \Delta D - M_0^{-1}D_0\Delta M||\dot{q}| + |\Delta G - M_0^{-1}G_0\Delta M| + |B(q)| + |d(t)|] - |M_0^{-1}\Delta M|(k_{P\ell}|\dot{e}| + K_{i\ell}|e| + K_{d\ell}|\ddot{q}_d|)\} - s_\ell^T K_{d\ell}(M_0 + \Delta M)u_r \tag{36}$$

to satisfy the inequality in (34), the reaching control law should be considered as:

$$u_r(t) = sign(S_\ell(t))[K_{d\ell}(M_0 + \Delta M_l)]^{-1}.\{[|(-\Delta M_h^{-1}\Delta V_h - \Delta M_h^{-1}\Delta D_h - D_0\Delta M_l^{-1} - V_0\Delta M_l^{-1})||\dot{q}| + |(\Delta M_h^{-1}\Delta G_h - G_0\Delta M_l^{-1})| + K_{d\ell}|d(t)| + K_{d\ell}|B(q)|] - |M_0\Delta M_h|(K_{p\ell}|\dot{e}| + K_{i\ell}|e| + K_{d\ell}|\ddot{q}_d|)\} \tag{37}$$

where, the maximum values of $\Delta M_h, \Delta M_l$, ΔD_h and ΔD_l are specified based on limitations of the actuators.

Remark 1. Note that signum function which appears in SMC controllers can cause chattering phenomena, or high-frequency oscillations of control variables. This problem can be avoided by replacing discontinuous signum

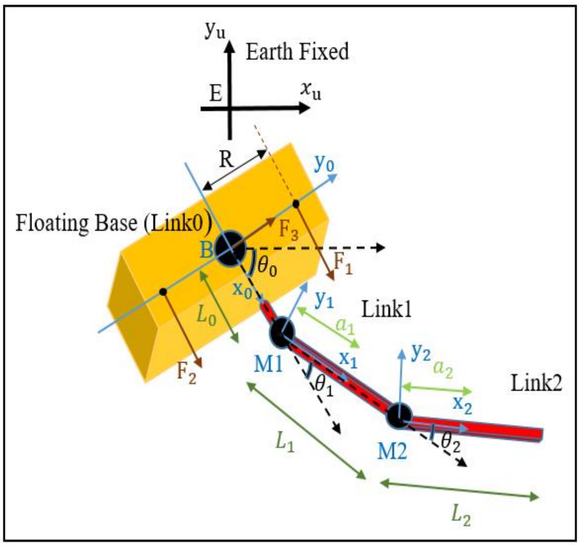

Fig. 1. Configuration of an UVMS

Table 1. Structure Parameter

Parameter	Definition	Value	Unit	Parameter	Definition	Value	Unit
L_0	Length	0.1	m	L_{z2}	Height(z axis)	0.12	m
L_1	Length(y axis)	0.25	m	a_1	Center of gravity	0.125	m
L_2	Length(y axis)	0.25	m	a_2	Center of gravity	0.125	m
L_{x0}	Width(x axis)	0.2	m	m_0	Mass	26.04	Kg
L_{x1}	Width(x axis)	0.04	m	m_1	Mass	4.25	kg
L_{x2}	Width(x axis)	0.04	m	m_2	Mass	1.23	Kg
L_{y0}	Length(y axis)	0.81	m	ρ	Fluid density	1000	m/v
L_{z0}	Height(z axis)	0.42	m	R	Length from origin	0.3	m

Table 2. Controller parameters (Set Point 1)

Item	Value	Item	Value	Item	Value	Item	Value	Item	Value
k_{i_1}	0.095	k_{p_1}	0.00001	k_{d_1}	0.0068	k_{Dc_1}	300	k_{Pc_1}	100
k_{i_2}	0.095	k_{p_2}	0.00001	k_{d_2}	0.0068	k_{Dc_2}	300	k_{Pc_2}	100
k_{i_3}	0.092	k_{p_3}	0.00001	k_{d_3}	0.0065	k_{Dc_3}	300	k_{Pc_3}	98
k_{i_4}	0.09	k_{p_4}	0.00001	k_{d_4}	0.0061	k_{Dc_4}	150	k_{Pc_4}	105
k_{i_5}	0.09	k_{p_5}	0.00001	k_{d_5}	0.0061	k_{Dc_5}	150	k_{Pc_5}	105

function with appropriate continuous approximation, like: $sign(s_l) = tanh(s_l / \varphi_l)$

4. GENETIC ALGORITHM

Genetic algorithm (GA) is started with an initial population and thereafter generate successive populations using three basic operations: crossover, mutation and reproduction [22-25]. The main feature of GA in this paper is to transform the system output into a cost function in order to find the best values of the control parameters which minimizes the amount of control efforts and tracking error. This cost function is defined as:

$$J = \frac{1}{2}\int_0^\infty \left[q^T(t)\eta q(t) + u^T(t)\gamma u(t) \right] dt \tag{38}$$

in which η and γ are set as $\eta = 10^2\left[\mathbb{I}_{10\times10}\right], \gamma = 10^2\left[\mathbb{I}_{10\times10}\right]$. Finally, the parameters of the controller resulted from GA have been specified in Tables 2-5.

5. SIMULATION RESULTS

In this section, for open loop dynamic verification of the UVMS in Fig.1, the 3-D model of the system is generated by using the ADAMS software and the response is compared with the MATLAB mathematical model. Also, to depict the effectiveness and performance of the proposed robust controller on an UVMS model, two cases are considered. The first one is the set point control of the system. The second simulation considers manipulation for predefined trajectory tracking. The UVMS dynamic parameters for simulation are set as Table.1.

5.1. Open Loop Dynamic Verification

For dynamic verification of the system, the following two

Table 3. Controller parameters (Set Point 2)

Item	Value	Item	Value	Item	Value
k_{s1_1}	20	k_{s2_1}	0.5	φ_1	0.0008
k_{s1_2}	20	k_{s2_2}	0.5	φ_2	0.0008
k_{s1_3}	20	k_{s3_3}	0.5	φ_3	0.0008
k_{s1_4}	18	k_{s4_4}	0.6	φ_4	0.0009
k_{s1_5}	18	k_{s5_5}	0.6	φ_5	0.0009

Table 4. Controller parameters (Trajectory Tracking 1)

Item	Value	Item	Value	Item	Value	Item	Value	Item	Value
k_{i_1}	0. 5	k_{p_1}	0.0095	k_{d_1}	0.0068	k_{Dc_1}	220	k_{Pc_1}	15
k_{i_2}	0. 5	k_{p_2}	0.0095	k_{d_2}	0.0068	k_{Dc_2}	220	k_{Pc_2}	15
k_{i_3}	0.52	k_{p_3}	0.0092	k_{d_3}	0.0065	k_{Dc_3}	218	k_{Pc_3}	13
k_{i_4}	0.48	k_{p_4}	0.009	k_{d_4}	0.0061	k_{Dc_4}	225	k_{Pc_4}	16
k_{i_5}	0.48	k_{p_5}	0.009	k_{d_5}	0.0061	k_{Dc_5}	225	k_{Pc_5}	16

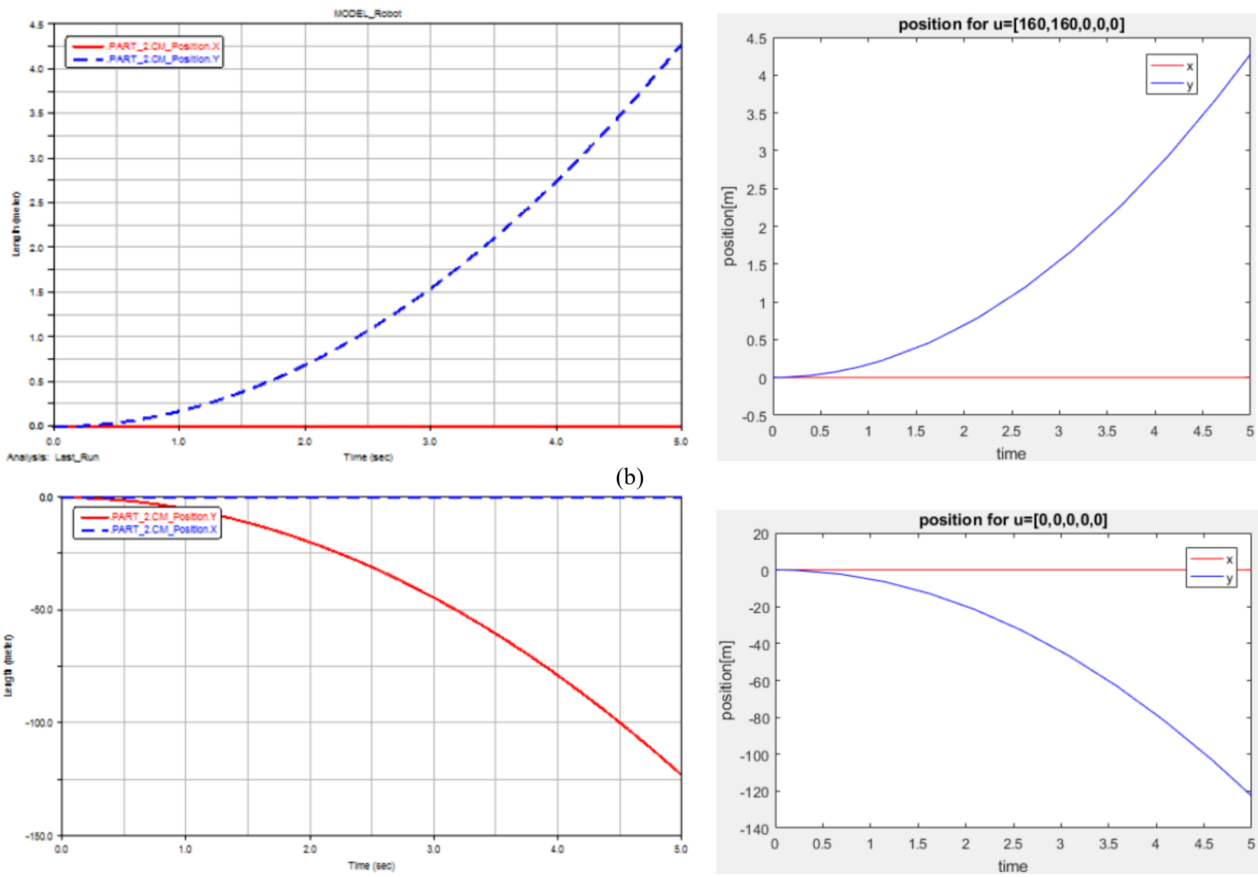

(a)

Fig. 2. Center of mass coordinates of the UVMS base for: (a) 1st case (b) 2nd case

cases are considered:

1st case: u= [0 0 0 0 0] ,

2nd case: u= [160 160 0 0 0]

Figs.2(a)-(b) and Figs.3(a)-(b) show the position and linear velocities of the UVMS base's center of mass for both cases. In each Figure, the left-hand drawing is the output of the ADAMS software and the right-hand drawing is the result of MATLAB model. These figures indicate the validity and conformity of the extracted dynamic model of the system.

5.2. Point-to-Point Control

In this section, the initial conditions of the UVMS are

Table 5. Controller parameters (Trajectory Tracking 2)

Item	Value	Item	Value	Item	Value
k_{s1_1}	22	k_{s2_1}	0.5	φ_1	0.006
k_{s1_2}	22	k_{s2_2}	0.5	φ_2	0.006
k_{s1_3}	25	k_{s3_3}	0.5	φ_3	0.007
k_{s1_4}	17	k_{s4_4}	0.5	φ_4	0.003
k_{s1_5}	18	k_{s5_5}	0.5	φ_5	0.003

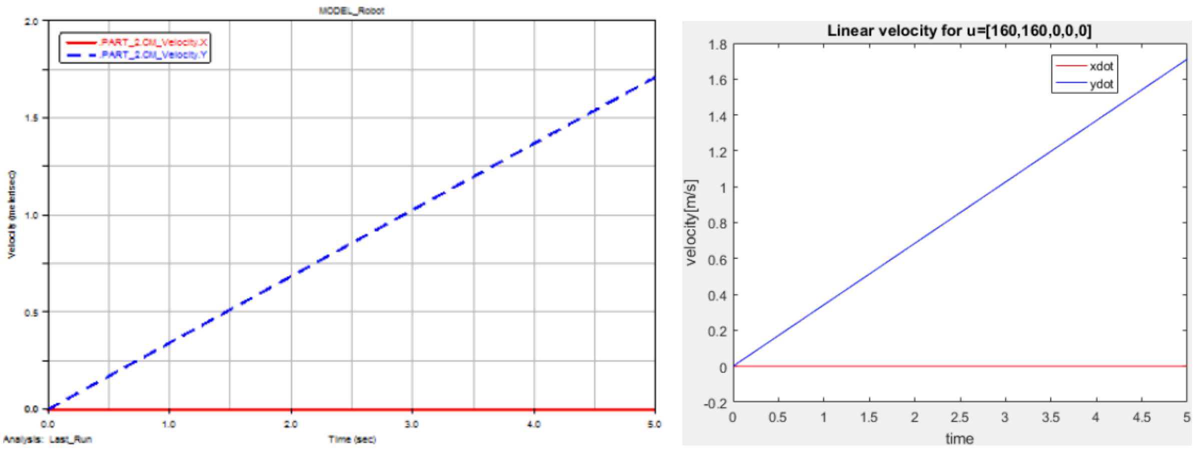

(b)

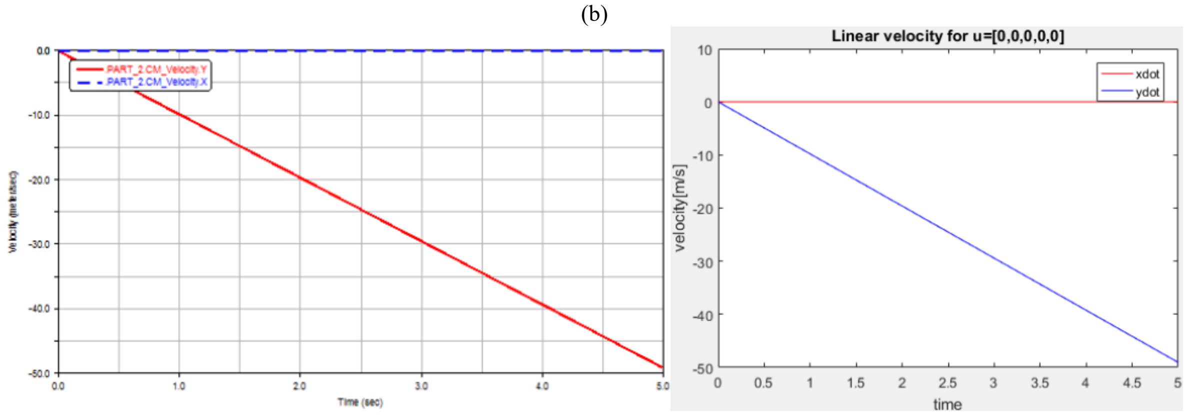

(a)

Fig. 3. Center of mass linear velocities of the UVMS base for: (a) 1st case (b) 2nd case

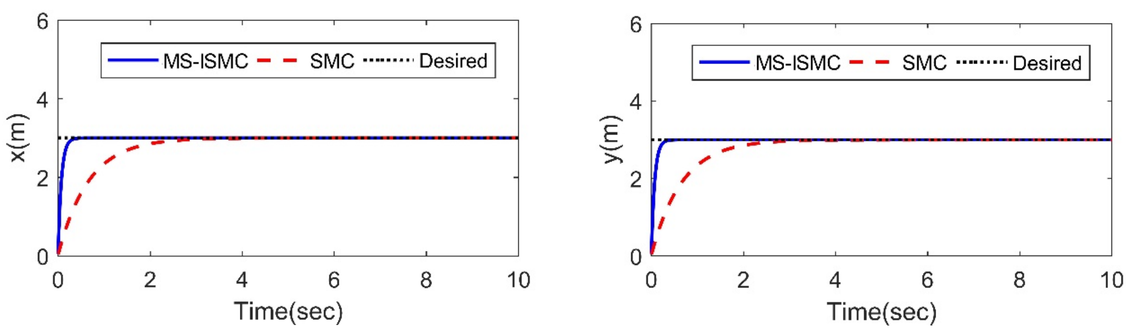

Fig. 4. Tracking simulation results: position (x ,y)

set as: $\theta_0(0)=\frac{\pi}{2}, \theta_1(0)=\frac{\pi}{6}, \theta_2(0)=\frac{\pi}{3}$, $x(0)=0.05$ and $y(0)=0.05$. In the first simulation, the desired set point is $[\theta_0, \theta_1, \theta_2, x, y,]=[0,0,0,3,3]$. The system uncertainties are considered as 15% of the actual values (i.e., the system model works with 85% of real values) and the uncertain conditions are set as $\Delta\alpha_i = 0.0859$ and $\Delta\beta_{ii} = 1.718$.

Assume that, the unknown external disturbance is

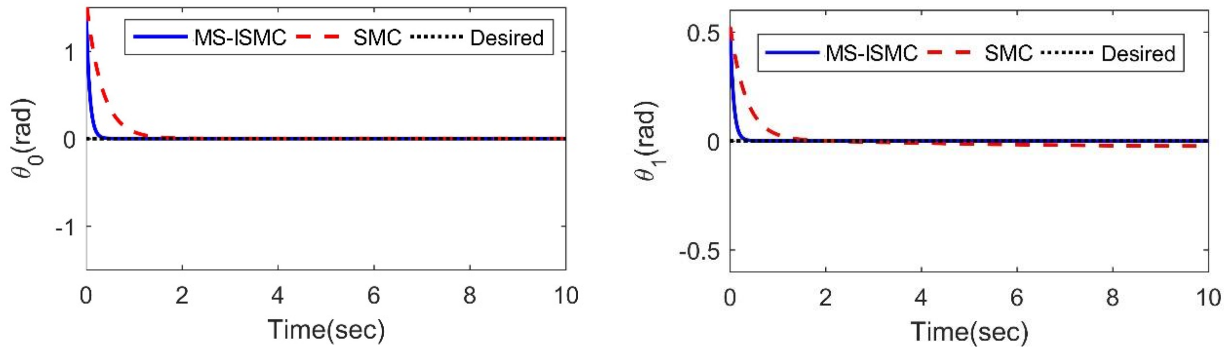

Fig. 5. Tracking simulation results: joint angles ()

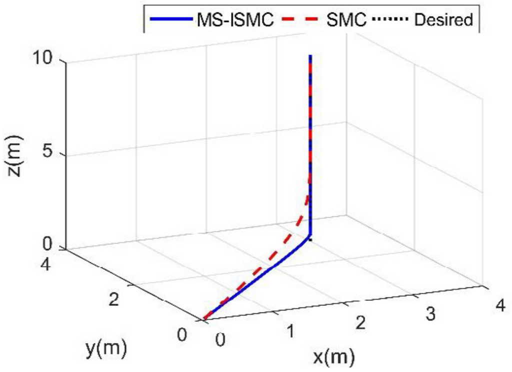

Fig. 6. Global trajectory of the UVMS position in 3-D space

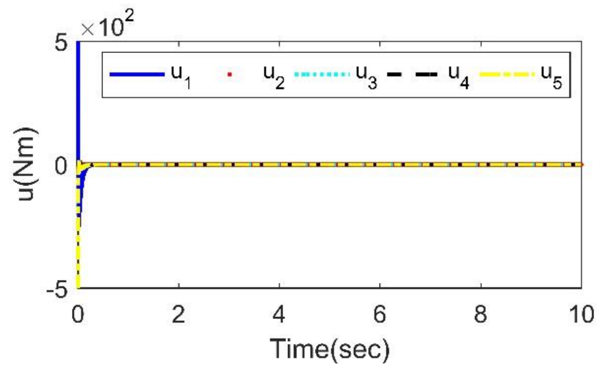

Fig. 7. Control inputs of UVMS

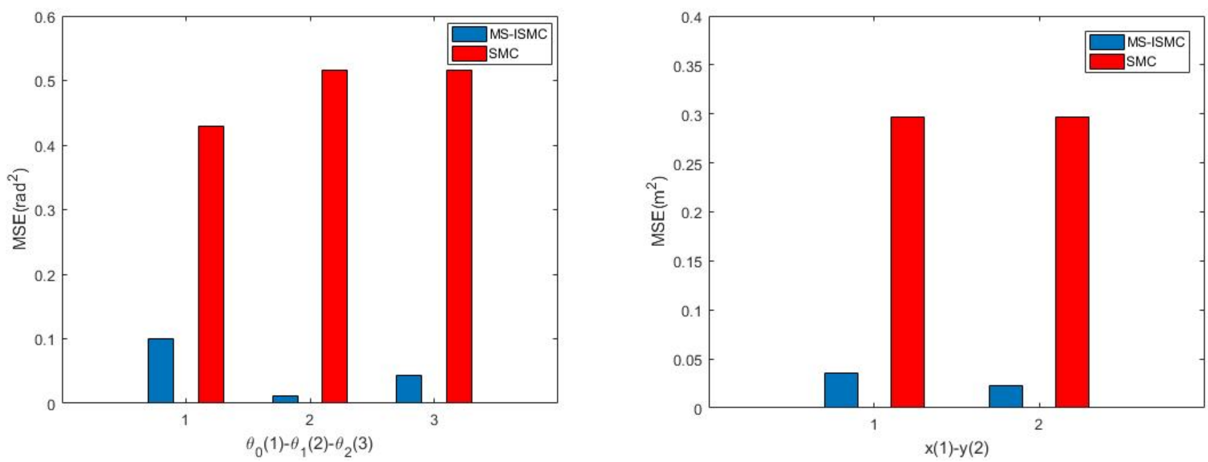

Fig. 8. Mean Square Error of positions and joint angles

described as: $(t)=0.5\sin\left(\frac{\pi(t-20)}{20}\right)$. Also, parameters of the proposed controller are listed in Tables.2 and 3. Now, the simulation results can be seen in Figs. 4–8. In these figures, the results of the proposed controller are compared with the conventional sliding mode controller.

The position and joint angles of the floating base and manipulator system in presence of external disturbance are depicted in Figs.4 and 5. As it can be seen, the controller stabilizes the system within a short duration.

Fig.6 shows 3-D trajectory of UVMS. It is evident that the system performs well and follows the desired set point in three dimensions. The control efforts are also shown in Fig.7.

Fig.8 compares Mean Square Error of the system variables for the two methods. We can see that the MS-ISMC method has a greater performance in comparison with conventional SLC method.

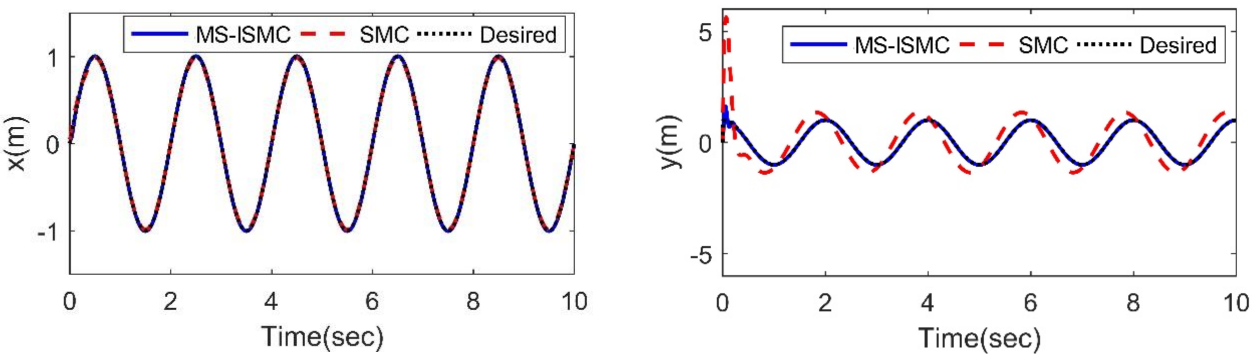

Fig. 9. Tracking simulation results: position (x ,y)

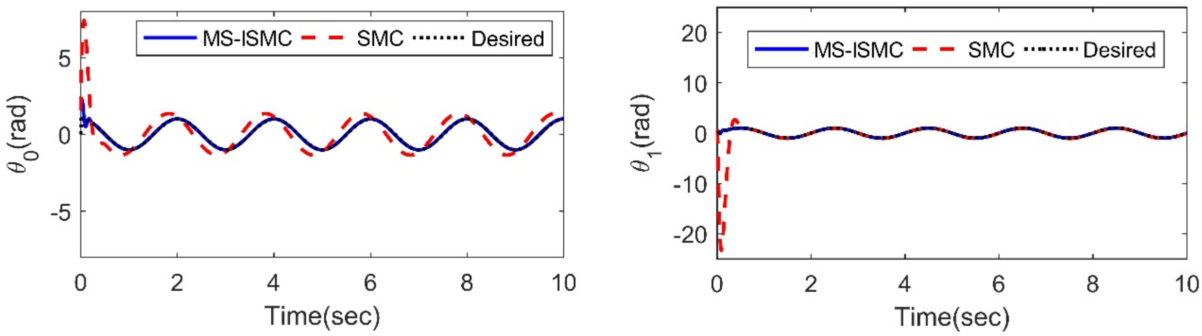

Fig. 10. Tracking simulation results: joint angles ()

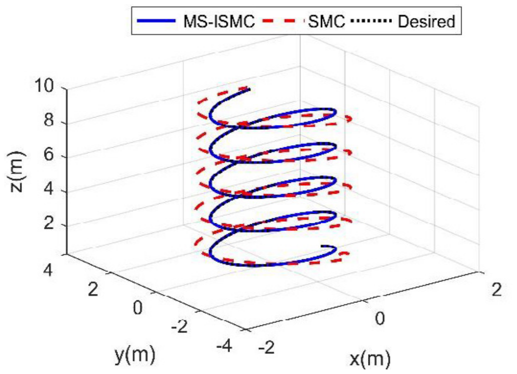

Fig. 11. Global trajectory of the UVMS position in 3-D space

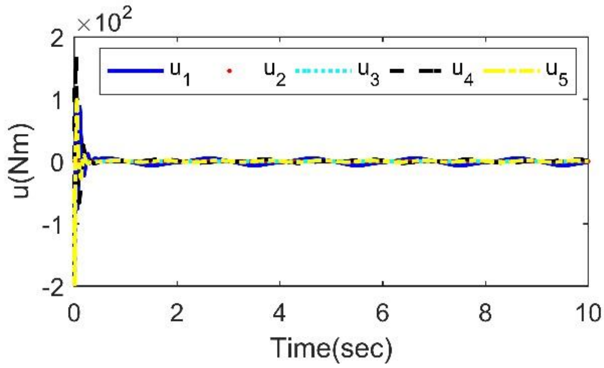

Fig.12. Control inputs of UVMS

5.3 Predefined Trajectory Tracking

In this section, a simulation is accomplished for a case in which the end-effector must track a predefined trajectory. The desired trajectory is defined as:

$$\left[\theta_0,\theta_1,\theta_2,x,y\right]=\left[cos\pi t, sin\pi t, 1-cos\pi t, sin\pi t, cos\pi t\right].$$

Other simulation conditions are similar to the previous section. Also, the parameters of proposed controller are listed in Table.4 and 5. The position of the floating base and the manipulator joint space variables in presence of external disturbance and with highly uncertain model are shown in Figs.9 and 10**.** These figures show that the controller is able to drive all the state variables back to the reference trajectories within few seconds.

To show the effectiveness of the proposed controller, trajectory of the whole vehicle in 3D space is displayed in Fig.11. It can be seen that the chattering phenomena is reduced by using the proposed controller and the tracking performance is fully acceptable. Also, Fig.12 shows that control scheme performs well and the control inputs are smooth.

Also, Fig.13 shows the Mean Square Error of all states for both methods. From these results, it can be observed that the tracking error converges to zero immediately and provides smooth control efforts by using the multi surface MS-ISMC controller as compared with the SLC controller.

6. CONCLUSION

In this study, a new multi surface integral SMC controller

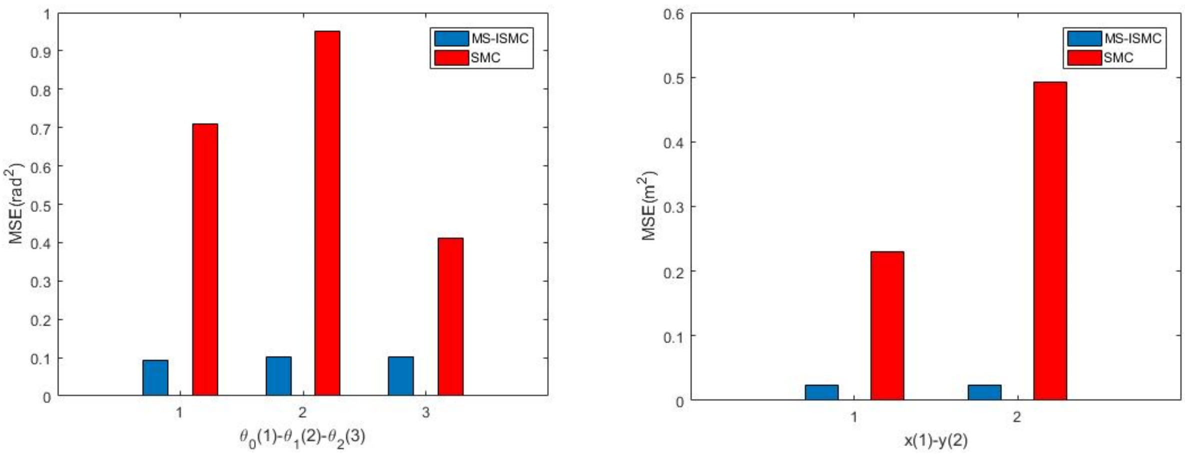

Fig. 13. Mean Square Error of positions and joint angles

developed for UVMS systems with floating base. The robustness of the proposed controller analyzed to address the position control in presence of some uncertainties and external disturbance. In this regard, the dynamic model of the UVMS system was extracted using Newton-Euler formulation with all hydrodynamic forces by Maple software. The multiple sliding surfaces of the controller guarantee the system robustness against the influence of unknown time-varying disturbances. At the next step, the control laws were extracted based on the second method of Lyapunov theory to ensure the stability of the overall closed loop control system. Eventually, the genetic algorithm was applied to regulate and optimize the parameters of proposed controller. Numerical simulations confirmed the effectiveness of the presented control scheme. In brief, the MS-ISMC method is more flexible than conventional SMC in tracking the reference trajectory and converges rapidly to an optimal value. It is notable that, all the state variables converge to the reference values with optimal control inputs, even if they change suddenly. The proposed controller in this research can be extended to a hybrid nonlinear controller in order to improve the performance. On the other hand, this approach is able to mitigate simultaneous actuator faults and exogenous disturbances if a proper observer will define (our future work).

REFERENCES

[1] T.W. Kim, J. Yuh, Development of a real-time control architecture for a semi-autonomous underwater vehicle for intervention missions, Control Engineering Practice, 12(12) (2004) 1521-1530.

[2] M. Santhakumar, Proportional-derivative observer-based backstepping control for an underwater manipulator, Mathematical Problems in Engineering, 2011 (2011) 1-18.

[3] J. Kim, W.K. Chung, J. Yuh, Dynamic analysis and two-time scale control for underwater vehicle-manipulator systems, in: 2003 IEEE/RSJ International Conference on Intelligent Robots and Systems, IEEE, Las Vegas, NV, USA, 2003, pp. 577-582.

[4] G. Antonelli, S. Chiaverini, Task-priority redundancy resolution for underwater vehicle-manipulator systems, in: 1998 IEEE International Conference on Robotics and Automation, IEEE, Leuven, Belgium, 1998, pp. 768-773.

[5] B.H. Jun, H.W. Shim, P.M. Lee, Approximated generalized torques by the hydrodynamic forces acting on legs of an underwater walking robot, International Journal of Ocean System Engineering, 1(4) (2011) 222-229.

[6] S. Mohan, J. Kim, Indirect adaptive control of an autonomous underwater vehicle-manipulator system for underwater manipulation tasks, Ocean Engineering, 54 (2012) 233-243.

[7] Y. Dai, S. Yu, Design of an indirect adaptive controller for the trajectory tracking of UVMS, Ocean Engineering, 151 (2018) 234-245.

[8] N. Sarkar, T.K. Podder, Coordinated motion planning and control of autonomous underwater vehicle-manipulator systems subject to drag optimization, IEEE Journal of Oceanic Engineering, 26(2) (2001) 228-239.

[9] G. Antonelli, F. Caccavale, C. S., Adaptive tracking control of underwater vehicle-manipulator systems based on the virtual decomposition approach, IEEE Transactions on Robotics and Automation, 20(3) (2004) 594-602.

[10] B. Xu, S.R. Pandian, M. Inoue, N. Sakagami, S. Kawamura, Model-based sliding mode control of underwater robot manipulators, International Journal of Offshore and Polar Engineering, 16(3) (2006) 210-217.

[11] H.N. Esfahani, V. Azimirad, M. Zakeri, Sliding mode-pid fuzzy controller with a new reaching mode for underwater robotic manipulators, Latin American applied research, 44(3) (2014) 253-258.

[12] F. Piltan, N. Sulaiman, A. Gavahian, S. Soltani, S. Roosta, Design mathematical tunable gain PID-like sliding mode fuzzy controller with minimum rule base, International Journal of Robotic and Automation, 2(3) (2011) 146-156.

[13] P.S. Londhe, M. Santhakumar, B.M. Patre, L.M. Waghmare, Task space control of an autonomous underwater vehicle manipulator system by robust single-input fuzzy logic control scheme, IEEE Journal of oceanic engineering, 42(1) (2016) 13-28.

[14] P.S. Londhe, S. Mohan, B.M. Patre, L.M. Waghmare, Robust task-space control of an autonomous underwater vehicle-manipulator system by PID-like fuzzy control scheme with disturbance estimator, Ocean Engineering, 139 (2017) 1-13.

[15] Y. Wang, S. Jiang, B. Chen, H. Wu, Trajectory tracking control of underwater vehicle-manipulator system using discrete time delay estimation, IEEE Access, 5 (2017) 7435-7443.

[16] Y. Wang, B. Chen, H. Wu, Nonlinear robust control of underwater vehicle-manipulator system based on time delay estimation, in: 14th International Conference on Ubiquitous Robots and Ambient Intelligence (URAI), IEEE, Jeju, South Korea, 2017, pp. 119-123.

[17] L.K. Grunenfelder, G. Milliron, S. Herrera, I. Gallana, N. Yaraghi, N. Hughes, K. Evans-Lutterodt, P. Zavattieri, D. Kisailus, Ecologically driven ultrastructural and hydrodynamic designs in stomatopod cuticles, Advanced Materials, 30(9) (2018) 1705295.

[18] F. Alnaimat, E. Alhseinat, F. Banat, Electromagnetic separation of heat stable salt from gas sweetening amine, International Journal of Greenhouse Gas Control, 68 (2018) 256-268.

[19] J. Bae, J. Bak, S. Jin, T. Seo, J. Kim, Optimal configuration and parametric design of an underwater vehicle manipulator system for a valve task, Mechanism and Machine Theory, 123 (2018) 76-88.

[20] R. Babaie, A.F. Ehyaie, Robust optimal motion planning approach to cooperative grasping and transporting using multiple UAVs based on SDRE, Transactions of the Institute of Measurement and Control, 39(9) (2017) 1391-1408.

[21] R. Babaie, A.F. Ehyaei, Robust control design of a quadrotor UAV based on incremental hierarchical sliding mode approach, in: 2017 Iranian Conference on Electrical Engineering (ICEE), IEEE, Tehran, Iran, 2017, pp. 835-840.

[22] B. Nagaraj, N. Murugananth, A comparative study of PID controller tuning using GA, EP, PSO and ACO, in: 2010 International Conference On Communication Control And Computing Technologies, IEEE, Nagercoil, India, 2010, pp. 305-313.

[23] C.S. Chin, W.P. Lin, Robust genetic algorithm and fuzzy inference mechanism embedded in a sliding-mode controller for an uncertain underwater robot, IEEE/ASME Transactions on Mechatronics, 23(2) (2018) 655-666.

[24] X. Wang, T. Lu, P. Zhang, State generation method for humanoid motion planning based on genetic algorithm, International Journal of Advanced Robotic Systems, 9(1) (2012) 1-8.

[25] W. Zhao, D. Yu, Z. Hu, Parameters optimization for small helicopter highly controller based on genetic algorithm, in: World Automation Congress 2012, IEEE, Puerto Vallarta, Mexico, 2012, pp. 1-4.

HOW TO CITE THIS ARTICLE

M. Mahmoodi, A.F. Ehyaei, J. Ehyaei, Nonlinear Robust Tracking Control of an Underwater Vehicle-Manipulator System, AUT J. Elec. Eng., 52(2) (2020) 193-204.

DOI: 10.22060/eej.2020.17665.5324